Surface Micelles of Single Chain Amphiphiles Bearing Azobenzene

ARTICLE *in* LANGMUIR · SEPTEMBER 2002

Impact Factor: 4.46 · DOI: 10.1021/la020294x

Surface Micelles of Single Chain Amphiphiles Bearing Azobenzene

Bo Zou,[†,‡] Dengli Qiu,[†] Xueliang Hou,[†] Lixin Wu,[†] Xi Zhang,*[,†] Lifeng Chi,*[,‡] and Harald Fuchs[‡]

Key Lab of Supramolecular Structure and Materials, College of Chemistry, Jilin University, Changchun 130023, People's Republic of China, and Physikalisches Institute, Westfälische Wilhelms-Universität, D-48149 Münster, Germany

Received March 27, 2002. In Final Form: July 29, 2002

The aggregation behavior of amphiphile bearing azobenzene surfactant ($C_{12}AzoC_6N^+$) was investigated using both in-situ and ex-situ AFM techniques. For the four substrates used (mica, HOPG and hydrophilic and hydrophobic silicon), the surfactant exhibits different structures in each case. In addition, the effect of adding electrolyte and ethanol on the aggregation behavior of $C_{12}AzoC_6N^+$ was studied.

Introduction

Surfactants in bulk solution have been investigated widely because of their commercial utility and scientific interest. Usually, they can form mesoscopic structures such as micelles and vesicles. Studies of surfactants at interfaces have been a traditional though challenging topic in colloid chemistry and supramolecular science in the recent time, including mineral flotation, wetting, colloidal stability, suspension stabilization, detergency, and fluid penetration into a porous substrate.[1−4] The aggregation behavior of surfactants is usually complex and depends strongly on their structure and solution conditions. Initially, Gaudin et al.[5] proposed the existence of clusters of surfactant molecules at solid/liquid interfaces. Manne et al.[6,7] showed for the first time that atomic force microscopy (AFM)[8] could be used to observe the aggregates of a cationic surfactant at a variety of solid surfaces of hydrophilic or hydrophobic substrates in contact with aqueous micellar solutions. Most substrates used are the ordered cleavage planes of layered solids such as mica and highly ordered pyrolytic graphite (HOPG). The surface aggregation of cationic surfactants,[6,7,9−20] anionic surfactants,[21−24] nonionic surfactants,[25,26] and zwitterionic surfactants[25,27−29] has been studied widely. The roles of substrate,[9,10,13,17,26,29] surfactant concentration,[18] electrolyte type,[11,16,22] pH,[14] temperature,[13] and ethanol[12] in determining the shape of the surface aggregates have also been examined systematically. For example, Liu et al.[13] have studied the aggregation behavior of a series of cationic C_nTAB surfactants by in-situ AFM for both hydrophilic silica and mica substrates. For a hydrophilic silica substrate, C_{14}TAB and C_{16}TAB adsorbed as spherical structures, whereas C_{18}TAB and C_{20}TAB formed flat layers. For a mica substrate, C_{12}TAB and C_{14}TAB adsorbed as cylindrical structures, whereas C_{16}TAB, C_{18}TAB, and C_{20}TAB formed flat layers. Zou et al.[30,31] have studied the 2D aggregate geometry of azobenzene containing bolaform amphiphiles after adsorption at a mica/aqueous solution interface through ex-situ AFM. The observed ordered stripes have a repeat spacing of 10 nm, and the ordered region extends over macroscopic areas. It is well-known that the surface micelles of conventional surfactants are only stable in solution. However, the surface micelles of bolaform amphiphile bearing azobenzene are stable even after drying. It is believed that a $\pi-\pi$ stacking interaction among the mesogenic groups of azobenzene plays an important role in stabilizing the surface nanostructures. In line with this research, herein we attempt to study the surface aggregation of a single chain quaternary ammonium surfactant containing azobenzene. The main

* To whom correspondence should be addressed. Xi Zhang: fax, +86-431-8923907; e-mail, xi@jlu.edu.cn. Lifeng Chi: fax, +49-251-8333602; e-mail, chi@uni-muenster.de.

† Jilin University.

‡ Westfälische Wilhelms-Universität.

(1) Ringsdorf, H.; Schlarb, B.; Venzmer, J. *Angew. Chem., Int. Ed. Engl.* **1988**, *23*, 113.
(2) Ahlers, M.; Müller, W.; Reichert, A.; Ringsdorf, H.; Venzmer. J. *Angew. Chem., Int. Ed. Engl.* **1990**, *29*, 1269.
(3) Kunitake, T. *Angew. Chem., Int. Ed. Engl.* **1992**, *31*, 709.
(4) Lehn, J. M. *Supramolecular Chemistry—Concepts and Perspectives;* VCH: Weinheim, 1995.
(5) Gaudin, A. M.; Fuerstenau, D. W. *Trans. AIME* **1955**, *202*, 958.
(6) Manne, S.; Cleveland, J. P.; Gaub, H. E.; Stucky, G. D.; Hansma, P. K. *Langmuir* **1994**, *10*, 4409.
(7) Manne, S.; Gaub, H. E. *Science* **1995**, *270*, 1480.
(8) Binnig, G.; Quate, C. F.; Gerber, C. *Phys. Rev. Lett.* **1986**, *56*, 930.
(9) Manne, S.; Schäffer, T. E.; Huo, Q.; Hansma, P. K.; Morse, D. E.; Stucky, G. D.; Aksay, I. A. *Langmuir* **1997**, *13*, 6382.
(10) Jaschke, M.; Butt, H. J.; Gaub, H. E.; Manne, S. *Langmuir* **1997**, *13* (3), 1381.
(11) Lamont, R. E.; Ducker, W. A. *J. Am. Chem. Soc.* **1998**, *120*, 7602.
(12) Wall, J. F.; Zukoski, C. F. *Langmuir* **1999**, *15*, 7432.
(13) Liu, J. F.; Ducker, W. A. *J. Phys. Chem. B* **1999,** *103*, 8558.
(14) Ducker, W. A.; Wanless, E. J. *Langmuir* **1999**, *15*, 160.
(15) Patrick, H. N.; Warr, G. G.; Manne, S.; Aksay, I. A. *Langmuir* **1999**, *15*, 1685.
(16) Subramanian, V.; Ducker, W. A. *Langmuir* **2000**, *16*, 4447.
(17) Schulz, J. C.; Warr, G. G. *Langmuir* **2000**, *16*, 2995.
(18) Velegol, S. B.; Fleming, B. D.; Biggs, S.; Wanless, E. J.; Tilton, R. D. *Langmuir* **2000**, *16*, 2548.
(19) Davey, T. W.; Warr, G. G.; Almgren, M.; Asakawa, T. *Langmuir* **2001**, *17*, 5283.
(20) Liu, J. F.; Min, G.; Ducker, W. A. *Langmuir* **2001**, *17*, 4895.
(21) Wanless, E. J.; Ducker, W. A. *J. Phys. Chem.* **1996**, *100*, 3207.
(22) Wanless, E. J.; Ducker, W. A. *Langmuir* **1997**, *13*, 1463.
(23) Jaschke, M.; Butt, H. J.; Gaub, H. E.; Manne, S. *Langmuir* **1997**, *13* (3), 1381.
(24) Wanless, E. J.; Davey, T. W.; Ducker, W. A. *Langmuir* **1997**, *13*, 4223.
(25) Grant, L. M.; Ducker, W. A. *J. Phys. Chem. B* **1997**, *101*, 5337.
(26) Grant, L. M.; Tiberg, F.; Ducker, W. A. *J. Phys. Chem. B* **1998**, *102*, 4288.
(27) Ducker, W. A.; Wanless, E. J. *Langmuir* **1996**, *12*, 5915.
(28) Wolgemuth, J. L.; Workman, R. K.; Manne, S. *Langmuir* **2000**, *16*, 3077.
(29) Ducker, W. A.; Grant, L. M. *J. Phys. Chem.* **1996**, *100*, 11508.
(30) Gao, S.; Zou, B.; Chi, L. F.; Fuchs, H.; Sun, J. Q.; Zhang, X.; Shen, J. C. *Chem. Commun.* **2000**, 1273.
(31) Zou, B.; Wang, L. Y.; Wu, T.; Zhao, X. Y.; Wu, L. X.; Zhang, X.; Gao, S.; Gleiche, M.; Chi, L. F.; Fuchs, H. *Langmuir* **2001**, *17*, 3682.

10.1021/la020294x CCC: $22.00
Published on Web 09/17/2002

Chart 1. Chemical Structure of Single Chain Amphiphiles Bearing Azobenzene

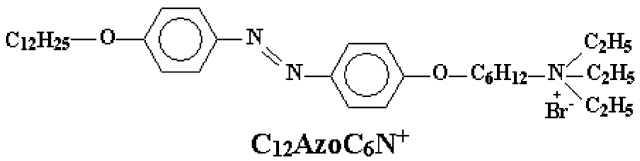

$C_{12}AzoC_6N^+$

purpose is to investigate, by means of in-situ and ex-situ AFM, how the different factors such as surfactant concentration, substrates, electrolyte, and ethanol influence the formation and morphology of surface micelles.

Experimental Section

The surfactant containing azobenzene used in this work was $C_{12}AzoC_6N^+$ (Chart 1), the synthesis of which has been published previously.[3,32] Sodium iodide (NaI, Aldrich, 99.99+%) and ethanol (Aldrich, AR) were used in this study. Water was purified by a Milli-Q system (Milli-Pore) with a resulting conductivity of 18.2 MΩ cm^{-1} at room temperature.

In this study, the adsorption of micelles at different solid substrates is studied systematically. We examined the adsorption of $C_{12}AzoC_6N^+$ on hydrophilic and hydrophobic silicon wafers (silicon wafers were purchased from Wafer Net GmbH, Germany), muscovite mica (purchased from PLANO W. Plannet GmbH, Germany), and HOPG (SPI-2, purchased from Structure Probe). Mica and HOPG was freshly cleaved for use.

Silicon wafers were cleaned by ultrasonic stirring in toluene, acetone, ethanol, and Milli-Q water (15 min in each). Then the wafers were dried with pure nitrogen, exposed to plasma for 5 min (TePla 100-E plasma system, 300W), and washed thoroughly using Milli-Q water. In this way, silicon wafers with good hydrophilicity were obtained. Immersing the hydrophilic silicon wafers in a 1% HF aqueous solution for 1 min, and washing with Milli-Q water, gave silicon wafers with good hydrophobicity.

Images were captured in-situ and ex-situ at the solid/liquid interface using the commercial instruments Nanoscope III and IIIa AFM Multimode (Digital Instruments, CA) at room temperature. Silicon cantilevers (Park Scientific, CA) with nominal spring constants of 0.06 N/m for tapping mode in fluid (f = 20−35 kHz) and silicon cantilevers (Nanosensors GmbH & Co. KG, Germany) for tapping mode in air were used (f = 200−300 kHz). An E scanner was selected for Multimode. Phase and height images are presented. Scan rates varied from 1 to 4 Hz, and integral and proportional gains, from 0.2 to 1. To obtain surface micelles on mica, a freshly cleaved mica sheet was immersed into an aqueous solution of the amphiphile at the appropriate concentrations.

For in-situ measurements, amphiphile solutions of the appropriate concentrations were injected into the liquid cell and allowed to equilibrate for at least 1 h before the imaging. In between the different concentrations, the liquid cell was washed by the new solution 10 times (each time over 30 s). The solution was held within the liquid cell by an O-ring, which was rinsed with Milli-Q water and dried under a nitrogen flow before use. In-situ AFM images of surfactant aggregates were obtained with tapping mode in fluid. Sometimes an external feedback circuit was used in order to obtain stable images and better resolution in liquid.[33,34] For ex-situ measurements, the substrate was taken out after adsorption for 30 min, and dried for approximately 1−2 h in a desiccator (P_2O_5). Ex-situ AFM images of surfactant aggregates were obtained with tapping mode in air. Images were minimally flattened, and a single low-pass filter to diminish high-frequency noise was used to facilitate data analysis. The spacing of the observed stripes and the diameter of the spheres were determined from section analysis. The 2D spectrum was obtained by a Fourier transform.

(32) Shimomura, M.; Ando, R.; Kunitake, T. *Ber. Bunsen-Ges. Phys. Chem.* **1983**, *87*, 1134.
(33) Anczykowski, B.; Cleveland, J. P.; Krueger, D.; Elings, V.; Fuchs, H. *Appl. Phys. A* **1998**, *66*, 885.
(34) Chi, L. F. *Appl. Phys. A* **1999**, *68*, 203.

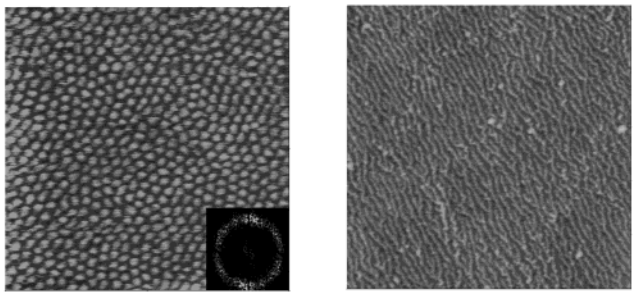

Figure 1. (a) In-situ AFM image (500 nm × 500 nm) of $C_{12}AzoC_6N^+$ adsorbed at a mica/aqueous solution interface. The concentration is 1.0×10^{-4} M. The inset is a 2D Fourier transform spectrum. (b) Ex-situ AFM image (1 μm × 1 μm) of $C_{12}AzoC_6N^+$ on a mica sheet. Nanosized branchlike stripes are formed by immersion of the mica sheet into an aqueous solution of $C_{12}AzoC_6N^+$ with a concentration of 1.0×10^{-4} M.

The critical micelle concentration (cmc) of the aqueous solution of $C_{12}AzoC_6N^+$ was determined from the concentration dependence of the fluorescence spectra recorded on a Shimadzu RF spectrometer. We used the fluorescence probe method (0.5 μM pyrene in this case) to measure the cmc, and from the sharp increase in the I_3/I_1 ratio we conclude that the cmc was approximately 4.2×10^{-5} M. The cmc of $C_{12}AzoC_6N^+$ at the liquid/substrate interface (surface cmc in brief) was determined from in-situ AFM images, as the concentration for which the aggregation behavior changed.

Results and Discussion

1. Concentration Effect. Concentration is a very important factor for surfactant adsorbing at the solid/liquid interface. In-situ AFM reveals that $C_{12}AzoC_6N^+$ forms spherical micelles on a mica surface. Figure 1a shows a 500 nm × 500 nm image of micelles with an approximately circular cross section at the interface between mica and a 1.0×10^{-4} M $C_{12}AzoC_6N^+$ aqueous solution. This concentration is higher than the cmc. The Fourier transform of the image is a circular ring, which indicates that there is a preferred separation between the centers of the micelles but no preferred orientation. The diameter of the spherical micelles is about 14 nm. To investigate a possible concentration dependence, the $C_{12}AzoC_6N^+$ concentration was varied systematically from 1.0×10^{-4} to 1.0×10^{-6} M. It was found that the spherical micelles are formed for a concentration of 1.0×10^{-5} M and above. The in-situ AFM images are the same as those shown in Figure 1a. Therefore, the surface cmc of $C_{12}AzoC_6N^+$ is $^1/_2$ the bulk cmc for a mica surface. This is understandable if we differentiate between the surface and bulk concentrations. As pointed out by Ducker,[13] surface forces cause a decrease in the concentration-independent part of the chemical potential and thus a greater concentration at the surface rather than in the bulk. Therefore, the surface cmc is usually lower than the bulk cmc. Gradually decreasing the concentration of $C_{12}AzoC_6N^+$ below the surface cmc, for example, 1.0×10^{-6} M, we only observe flat structures. Thus, for surfactant concentrations below the surface cmc, surface micelles at the solid/liquid interface cannot form.

In contrast, ex-situ AFM reveals that $C_{12}AzoC_6N^+$ forms branchlike stripes at the mica surface, as shown in Figure 1b. The concentration of the $C_{12}AzoC_6N^+$ aqueous solution is maintained at 1.0×10^{-4} M in this case. From ex-situ AFM, the width of the branchlike stripes is about 16 nm. When the concentration of $C_{12}AzoC_6N^+$ is gradually decreased down to its bulk cmc, branchlike stripes are

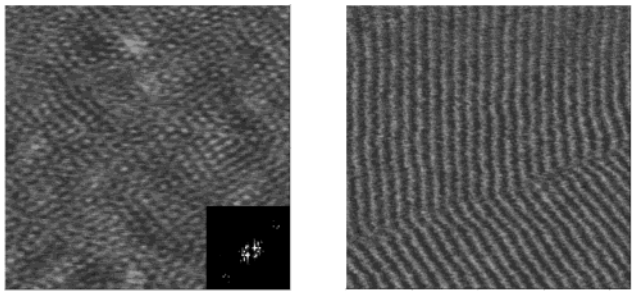

Figure 2. (a) In-situ AFM image (500 nm × 500 nm) of $C_{12}AzoC_6N^+$ adsorbed at a hydrophilic silica/aqueous solution interface. The concentration is 1.0×10^{-5} M. The inset is a 2D Fourier transform spectrum. (b) In-situ AFM image (860 nm × 860 nm) of $C_{12}AzoC_6N^+$ adsorbed at a HOPG/aqueous solution interface. The concentration is 2.0×10^{-5} M.

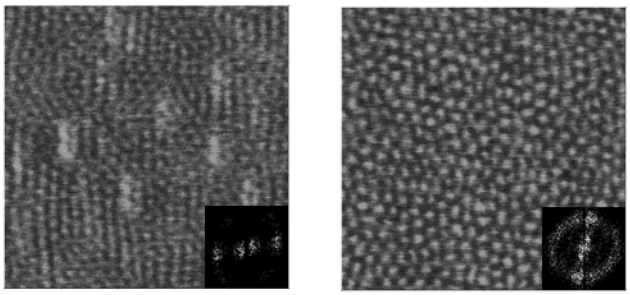

Figure 3. Effect of adding NaI into $C_{12}AzoC_6N^+$ aqueous solution. The concentration of $C_{12}AzoC_6N^+$ is 1.0×10^{-4} M. The concentration of NaI is 5.0×10^{-5} M. Insets are 2D Fourier transform spectra. (a) In-situ AFM image (500 nm × 500 nm) of $C_{12}AzoC_6N^+$ adsorbed at a mica/aqueous solution interface. (b) In-situ AFM image (500 nm × 500 nm) of $C_{12}AzoC_6N^+$ adsorbed at a hydrophilic silica/aqueous solution interface.

still observed. The difference between in-situ and ex-situ AFM images could be explained by the instability of the micelles. In other words, the surface micelles that formed by the interfacial adsorption of $C_{12}AzoC_6N^+$ at the mica surface are destroyed upon drying. Because of the existence of energetically preferred attachment sites along a particular orientation relative to the mica crystal lattice,[35] some spherical micelles collapsed and formed branchlike stripes. For concentrations below the bulk cmc, for example, 1.0×10^{-5} M, ex-situ AFM reveals that $C_{12}AzoC_6N^+$ forms non-close-packed spheres in patchy-like domains.

2. Substrate Effect. Surface aggregation of surfactants strongly depends on the substrate. For a hydrophilic silicon wafer instead of mica as the substrate, and concentrations above 1.0×10^{-5} M, in-situ AFM reveals that $C_{12}AzoC_6N^+$ forms spherical micelles of 14 nm in diameter on the substrate surface (Figure 2a). The Fourier transform of the image indicates a preferred separation between the centers of the micelles. In other words, the micelles are well packed locally. For concentrations below 1.0×10^{-5} M, flat structures at the substrate/solution interface are observed. Therefore, for a hydrophilic silicon substrate, the surface cmc of $C_{12}AzoC_6N^+$ is 1.0×10^{-5} M, which is similar to the case of a mica substrate. Upon drying, ex-situ AFM reveals the presence of only a few spherical aggregates with a completely random distribution over the surface. Their average diameter is larger than that in in-situ AFM images. Thus, drying also destroys the micelle structure for a hydrophilic silicon substrate.

In the case of a hydrophobic silicon substrate, in-situ AFM reveals that $C_{12}AzoC_6N^+$ forms a flat film on the substrate surface. The surfactant aggregates at a hydrophobic substrate have a lower curvature.[26] This may be due to strong affinity between the substrate and the surfactant, leading to the flattening of the surface micelles to increase the contact area.[14] The alkyl chains assemble normal to the substrate surface, with the headgroups pointing away from the substrate. Thus, the surfactant forms flat sheets on hydrophobic silicon.

HOPG is also a hydrophobic substrate. However, the aggregation behavior on HOPG is more complicated than that on hydrophobic silicon. In-situ AFM images of $C_{12}AzoC_6N^+$ adsorbed at the HOPG/aqueous solution interface feature hemicylindrical structures for concentrations above $^1/_2$cmc. The width of the observed stripes is approximately 20 nm (Figure 2b), and the axis of the hemicylindrical structures is normal to the HOPG crystal lattice. The molecules lie with their molecular axis parallel to the HOPG lattice directions.[36] When the concentration is decreased to $^1/_2$cmc and below, only flat structures on the HOPG surface are observed. Thus, in this case the surface cmc of $C_{12}AzoC_6N^+$ is $^1/_2$ the bulk cmc. For both mica and hydrophilic silica substrates, the surface cmc is $^1/_2$ the bulk cmc, while, for the HOPG substrate, the surface cmc is $^1/_2$ the bulk cmc.

3. Electrolyte Effect. The adsorption of electrolyte onto the micelle surface can reduce repulsive headgroup interactions, thereby lowering the curvature of the micelles. [16] Sometimes this leads to the formation of less curved and more closely packed aggregates.[37] For NaI concentrations higher than 5.0×10^{-6} M, the $C_{12}AzoC_6N^+$ precipitates out. Therefore, the concentration of $C_{12}AzoC_6N^+$ was maintained at 1.0×10^{-4} M, and that of NaI, at 5.0×10^{-6} M, while different substrates were used in order to study the effect of electrolyte on the surface aggregation behavior.

For a mica substrate, in-situ AFM shows $C_{12}AzoC_6N^+$ forming spherical micelles in the presence of electrolyte (Figure 3a). The Fourier transform of the image is not a complete circle but two arcs, indicating a preferred orientation to some extent. The diameter of the spherical micelles does not change on addition of the electrolyte. From Figures 1a and 3a, it is seen that the randomly packed spherical surface micelles on the mica sheet become locally oriented, on addition of NaI into the $C_{12}AzoC_6N^+$ aqueous solution. In ex-situ AFM images, similar structures are observed in the absence and presence of the electrolyte. However, in the latter case the diameter of the spherical micelles is larger and the aggregate is not close-packed. This shows that the electrolyte can stabilize ionic surfactant micelles by binding to the micelle surface and screening the electrostatic repulsion between the ionic headgroups. The result is a well-ordered aggregation on the mica sheet.

Figure 3b shows an in-situ AFM image of $C_{12}AzoC_6N^+$ adsorbed at the hydrophilic silicon/aqueous solution interface. The Fourier transform of the image is a circular ring, indicating a preferred separation between the centers of the micelles but no preferred orientation. The diameter of the spherical micelles is the same as that in the absence of the electrolyte. From Figure 2a and Figure 3b, the well-

(35) Yang, H.; Kuperman, A.; Coombs, N.; Mamiche-Afara, S.; Ozin, G. A. *Nature* **1996**, *379*, 703.

(36) Cyr, D. M.; Venkataraman, B.; Flynn, G. W. *Chem. Mater.* **1996**, *8*, 1600.

(37) Israelachvili, J. N.; Mitchell, D. J.; Ninham, B. W. *J. Chem. Soc., Faraday Trans.* **1976**, *72*, 1525.

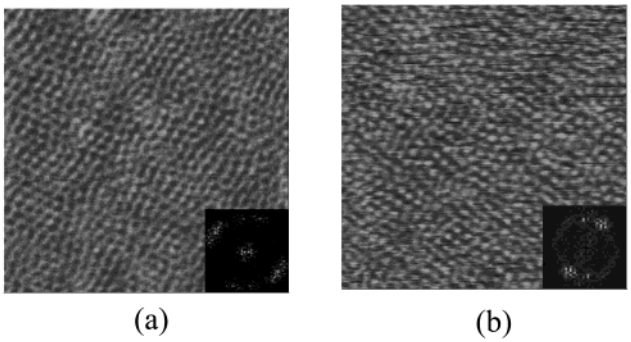

Figure 4. Effect of adding ethanol into $C_{12}AzoC_6N^+$ aqueous solution. The concentration of $C_{12}AzoC_6N^+$ is 1.0×10^{-4} M. The concentration of ethanol is 0.1 mL/mL. Insets are 2D Fourier transform spectra. (a) In-situ AFM image (500 nm × 500 nm) of $C_{12}AzoC_6N^+$ adsorbed at a mica/aqueous solution interface. (b) In-situ AFM image (500 nm × 500 nm) of $C_{12}AzoC_6N^+$ adsorbed at a hydrophilic silica/aqueous solution interface.

packed spherical surface micelles on the hydrophilic silicon substrate become randomly packed spheres, when NaI is added into the $C_{12}AzoC_6N^+$ aqueous solution. Therefore, the electrolyte decreases the array order on the hydrophilic silicon substrate.

Surface aggregation of $C_{12}AzoC_6N^+$ at the HOPG/aqueous solution interface was also studied by in-situ AFM. No characteristic structures were observed. It is possible that the electrolyte disables the physisorption of the micelles onto the HOPG surface.

4. Ethanol Effect. It is well-known that ethanol can decrease the cmc and increase the degree of ionization. It can change the ionization of the surface groups through competitive adsorption on the particle surface and change the hydrogen-bonded structure of water.[12]

An in-situ AFM image of $C_{12}AzoC_6N^+$ adsorbed at the mica/aqueous solution interface is shown in Figure 4a. The concentration of ethanol is 0.1 mL/mL. As in the case of adding electrolyte, adding ethanol has no effect on the diameter of the spherical micelles. For very high concentrations of ethanol, for example, 0.5 mL/mL, only flat structures are observed, indicating that excess ethanol may influence micelle aggregation behavior in solution and at the mica/solution interface. For low ethanol concentrations, for example, 0.01 mL/mL, a very similar in-situ AFM image to that of Figure 1a is obtained. This means that the ethanol effect can be neglected at low concentrations. Consequently, we selected an ethanol concentration of 0.1 mL/mL and studied the surface micelles of $C_{12}AzoC_6N^+$ on different substrates. Upon drying, ex-situ AFM reveals only some spherical aggregates with a completely random distribution over the surface. The average diameter of the aggregates is larger than that in in-situ AFM images. Thus, drying again destroys the micelle structure, as is the case for a hydrophilic silicon substrate. Ex-situ AFM images of $C_{12}AzoC_6N^+$ adsorbed on a mica sheet, after the addition of ethanol, feature faint branchlike stripes.

An in-situ AFM image of $C_{12}AzoC_6N^+$ adsorbed at the hydrophilic silicon/aqueous solution interface is shown in Figure 4b. For a hydrophilic silicon substrate, the result of adding ethanol is different from that of adding electrolyte. Both Figure 2a and Figure 4b feature a dot matrix; the diameter of the spheres is the same. Thus, we can conclude that ethanol has no obvious influence on the structure of the surface micelles of $C_{12}AzoC_6N^+$ adsorbed on the hydrophilic silicon substrate.

In-situ AFM images of the HOPG/aqueous solution interface show some hemicylindrical structures with short-range order. The width of the observed stripes is approximately 30 nm. Maybe the ethanol partly decreases the interaction between the physisorbed $C_{12}AzoC_6N^+$ and the HOPG surface and thus influences the hemicylindrical micelle aggregation.

Conclusion

In summary, the aggregation behavior of $C_{12}AzoC_6N^+$ was studied using in-situ and ex-situ AFM. The $C_{12}AzoC_6N^+$ tends to form spherical micelles in aqueous solution because ofo the hydrophobic effect. On a hydrophilic silicon wafer, the spherical micelles adsorb with a local preferred orientation. However, flat structures are observed in the case of a hydrophobic silicon substrate under the same conditions. On HOPG, the micelles have a semicylindrical shape, leading to a stripelike pattern in the AFM images. The aggregation behavior of $C_{12}AzoC_6N^+$ can be varied by adding electrolyte and ethanol to the buffer solution. Different substrates have different surface cmc values according to in-situ AFM evidence.

Acknowledgment. The research was funded by the Major State Basic Research Development Program (Grant No. G2000078102), Key Project of Ministry of Education, Natural Science Foundation of China; and a German−Chinese cooperation program supported by the state of North Rhine-Westphalia, Germany. X.Z. thanks DFG for support during his two-month visit at the Westfälische Wilhelms-Universität, Münster, Germany.

LA020294X